PCCP

Cite this: *Phys. Chem. Chem. Phys.*, 2012, **14**, 3280–3289

www.rsc.org/pccp

PERSPECTIVE

Analytical methods for separating and isolating magnetic nanoparticles

Jason R. Stephens, Jacob S. Beveridge and Mary Elizabeth Williams*

Received 19th September 2011, Accepted 12th January 2012
DOI: 10.1039/c2cp22982j

Despite the large body of literature describing the synthesis of magnetic nanoparticles, few analytical tools are commonly used for their purification and analysis. Due to their unique physical and chemical properties, magnetic nanoparticles are appealing candidates for biomedical applications and analytical separations. Yet in the absence of methods for assessing and assuring their purity, the ultimate use of magnetic particles and heterostructures is likely to be limited. In this review, we summarize the separation techniques that have been initially used for this purpose. For magnetic nanoparticles, it is the use of an applied magnetic flux or field gradient that enables separations. Flow based techniques are combined with applied magnetic fields to give methods such as magnetic field flow fractionation and high gradient magnetic separation. Additional techniques have been explored for manipulating particles in microfluidic channels and in mesoporous membranes. Further development of these and new analytical tools for separation and analysis of colloidal particles is critically important to enable the practical use of these, particularly for medicinal purposes.

Introduction

Particles that have at least one dimension less than 100 nm have size-dependent physical behaviors that uniquely differ from those of the bulk solid or the atomic species.[1,2] In the nanometre-size range, electrical, optical, and magnetic properties are significantly affected and highly dependent on size and structure.

The Pennsylvania State University, 104 Chemistry Building, University Park, PA 16802, USA. E-mail: mbw@chem.psu.edu; Fax: (814) 863-8404; Tel: (814) 865-8859

Developing methods for making size monodisperse nanoparticles (*i.e.* size variation $< 5\%$) has been centrally important because of the known variation of behaviour with size, however much of the effort to date has been focused on exerting synthetic control over the size and monodispersity of particles.[3–5] Organizing nanostructures into functional materials, for example with addressable nanoscopic components or as hybrid heterostructures, represents a significant challenge in nanoscience and is the current frontier for nanomaterials. With recent advancements in the synthesis of nanomaterials,[6,7] it is becoming feasible to draw analogy between atomic bond formation and

Jason R. Stephens

Jason R. Stephens earned his BS in Chemistry at LaSalle University in 2006. He is currently a 5th year graduate student completing his PhD in Chemistry at the Pennsylvania State in Mary Elizabeth Williams' laboratory. Jason has focused on the development of analytical techniques to purify, separate and analyze magnetic nanoparticles. He has studied the diffusive flux of nanoparticles through porous membranes to understand their transport in complex mesoporous systems such as the environment. Currently, he is investigating the formation of linked nanoparticle assemblies within a microfluidic device.

Jacob S. Beveridge

Jacob S. Beveridge received a BS in chemistry from Harding University (2007). He is currently a 5th year graduate student working toward his PhD with Professor Mary Elizabeth Williams in the Department of Chemistry at The Pennsylvania State University. His thesis research includes the development of analytical tools for analysis of magnetic nanomaterials. In this work, Jacob has developed differential magnetic catch and release (DMCR), which has been used for the separation, purification, and characterization of magnetic nanoparticles and hybrid nanostructures.

nanoparticle assembly.[8,9] However, in contrast to molecular syntheses, in reports of new nanoparticle and hybrid structures, little has been reported on complementary efforts to purify and isolate nanomaterials. There is an immediate need to develop and apply analytical methods to address this challenge, which is of growing importance for the isolation, investigation and application of new multiparticle hybrid structures.

Nanomaterials have been synthesized with unique properties as a result of their size,[10–12] shape,[13–16] material composition,[17–20] and surface modification.[21–23] The shifting focus toward the assembly of single nanoparticles or directed growth of high-order, multi-domain structures aims to produce hybrid structures with the combined properties of the nanoscale substituents. Hybrid structures containing one or more magnetic domains are of intense interest. These have potential industrial and biomedical applications, for example as photocatalytic materials, drug delivery vehicles, or plasmonic devices. Assembly approaches for producing the heterostructures include using nanoparticles as building blocks, which when linked together, with molecular linkers or a common solid-state interface, form complex structures.[24–26] In addition to the ways that individual particles are affected, polydispersity in heterostructures is especially problematic. Formation of higher order assemblies can be affected when there is variance in the size and surface chemistry in the particle population. A distribution in the types of particles present in the hybrid structure sample (*i.e.* single particles *versus* dimers, trimers, and higher order structures), leads to observed properties that are the ensemble average of the entire population. Without analytical separation and analysis tools, polydispersity can render nanoparticle heterostructures into nonstarters for their envisioned applications.

By reducing or eliminating the polydispersity of nanoparticles and heterostructures, it becomes increasingly feasible to tailor the properties and functions of hybrid nanostructured materials. This precision will ultimately be important in manufacturing, for example where only hybrid nanoparticles of a specific structure are useful for device performance. Further, it is likely that prior to approval for any medical application, nanomaterial purity will need to be validated. This remains an issue for even single nanoparticles (*i.e.* not hybrid materials). For example, individual nanoparticles prepared with several methods (*e.g.* reverse micelles,[27] thermal decomposition)[28] are often reported to possess a low degree of size polydispersity but for medicinal use, purity of the bulk sample would need to be confirmed. Indeed, the majority of particle samples would benefit both from post-synthetic purification and confirmation of purity, although surprisingly few methods exist to do so.

In this review, we briefly outline techniques for synthesizing magnetic particles and for determining their magnetic behaviours to provide a basic understanding of the types of materials that are commonly used and available. The remainder of this review describes recent developments in the purification and analysis of nanoparticles. These techniques generally employ applied magnetic and electric fields, mesoporous filtration, and chemical or biochemical purification as they pertain to studying magnetic nanomaterials for bioanalysis, drug delivery, and MRI contrast agents. This article is intended to provide some perspective of the need and current state of the field for magnetic nanoparticle separations: methods for the purification and analysis of magnetic nanoparticles are in their infancy, yet far outpace those for non-magnetic nanoparticles and heterostructures.

Mary Elizabeth Williams

Mary Elizabeth Williams is Associate Professor of Chemistry and Associate Dean for Undergraduate Education in the Eberly College of Science at The Pennsylvania State University. After earning her PhD in analytical chemistry at the University of North Carolina—Chapel Hill in 1999, she spent two years as a post-doctoral research associate at Northwestern University before beginning at Penn State in 2001. Williams' research group focuses on developing analytical methods for the separation and analysis of nanoparticles and hybrid particle structures, and on building and studying hetero-multimetallic assemblies for artificial photosynthesis, catalysis and molecular wires.

Magnetic nanoparticle synthesis

Magnetic nanoparticles are of intense interest for a variety of applications because their physical properties vary dramatically from their bulk counterparts. At diameters less than 20 nm, magnetic nanoparticles are commonly superparamagnetic at room temperature. That is, their magnetization is saturated in an external magnetic field, but in the absence of this field the magnetic moments are randomized by thermal fluctuations. Particle size, crystallinity, elemental composition and perhaps shape are all important in determining the superparamagnetism of a material. However general rules to predict the magnetic properties of a nanoparticle are difficult to define in part because model materials contain a population with variation in one or more of these properties. Nonetheless, due to their unique superparamagnetic properties, magnetic nanoparticles are promising for enhancing known properties of commercial materials and for use in biomedical applications. Below we briefly summarize the most common synthetic methods of magnetic nanoparticles and heterostructures, and compare the size variation typically reported for each.

Within the past decade, a wide array of magnetic nanoparticles of different composition and structure has been synthesized using wet chemical methods. The most common magnetic nanomaterials are the iron oxides (Fe_2O_3 and Fe_3O_4) and their corresponding ferrites (*e.g.* $CoFe_2O_4$, $MnFe_2O_4$, $NiFe_2O_4$, and $MgFe_2O_4$). Examples of transmission electron microscopy images of these are shown in Fig. 1. In addition, FePt, CoPt, and FePd nanoparticles are of interest because these possess high magneto-crystalline anisotropy and good chemical stability. Other metals and alloys such as Mn_3O_4, Co, Ni, α-Fe are less common because of either their rapid oxidation or potential for cytotoxicity.

According to theory developed by LaMer,[29] magnetic nanoparticles are synthesized in solution with separate nucleation and growth steps. Magnetic nanomaterials are typically made *via* thermal decomposition by a hot injection procedure wherein

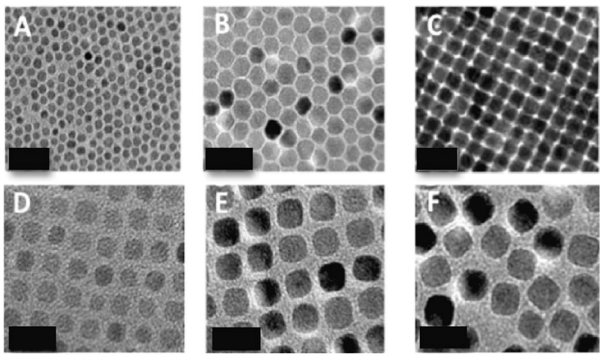

Fig. 1 Transmission electron microscope (TEM) images of samples obtained from the thermal decomposition synthesis of (**A–C**) 6 to 12 nm diameter Fe_3O_4 (reprinted with permission from Sun *et al. J. Am. Chem. Soc.* 2004, **126**, 279. Copyright 2004 American Chemical Society) and (**D–F**) 8–11 nm diameter $CoFe_2O_4$ (Gupta *et al. Chem. Mater.* 2009, **21**, 3458–3468. Copyright 2009 American Chemical Society). Scale bars are 20 nm.

burst nucleation is achieved by rapid introduction of reagents into the reaction vessel. Alternatively, a pre-mixed solution of precursors, surfactants, and solvent is heated to a specific temperature to initiate particle clustering and growth. A typical thermal decomposition method requires a metal precursor (*e.g.* $Fe(CO)_5$, $Co(acac)_2$, $Fe(acac)_3$) and surfactant (*e.g.* oleic acid and oleylamine) in an organic solvent with a high boiling point. Modification of the reaction parameters (*e.g.* pH, temperature, precursors, *etc.*) serves as a way to tune particle size, shape and therefore magnetic properties of the nanoparticles.

For example, Sun *et al.*[30] carried out high-temperature solution phase reaction of metal acetylacetonate (*i.e.* iron, cobalt, and manganese) in the presence of oleic acid and oleylamine to yield nanoparticles with varying diameter 3–20 nm ± 10% size disperse. Variation of reaction conditions or seed-mediated growth was used to decrease or increase the particle size, respectively. Synthesis of γ-Fe_2O_3 was reported by Hyeon *et al.*[31] by controlled oxidation of Fe nanoparticles using trimethylamine oxide as a mild oxidant. Sun *et al.*[32] prepared FePt nanoparticles with narrow size distributions (< 10% standard deviation) *via* decomposition of $Fe(CO)_5$ and simultaneous reduction of Pt(acetylacetonate) to make particles with up to 9 nm in diameter.

Two additional wet-chemical methods of synthesizing magnetic nanoparticles are co-precipitation and templated growth in micro-emulsions. One of the main challenges with these is defining ways to exert control over variance in size, since both typically generate particles with a broad size distribution. Each of these utilizes metal salts in aqueous solutions. Co-precipitation is a convenient way to synthesize iron oxide nanoparticles from aqueous Fe^{2+}/Fe^{3+} salt solutions by the addition of a base at low temperatures. The type of salt used (*e.g.* chloride, sulfate, nitrate), Fe^{2+}/Fe^{3+} ratio, reaction temperature, pH of the solution, and ionic strength all play roles in determining the size, shape, and composition of the nanoparticle sample.[33] Co-precipitation is the most straightforward and least costly method for magnetic particle synthesis, however yields nanoparticles that can be 10 to 200 nm in mean diameter with large size dispersity (10–30%, or more) and poor crystallinity compared to thermal decomposition.

Template synthesis of particles in microemulsions alternatively uses specific surfactants to form spherical or oblate micelles.[34,35] When the solvent is completely free of water, these are small and size polydisperse, however the presence of water produces large and surfactant aggregates with narrower size distributions. Nanoparticles synthesized using this method form within the water core of the micelle. Microemulsion synthesis thus affords better size control compared to co-precipitation, but the range of possible nanoparticle diameters is limited by the size of the micelle interior. As with co-precipitation, microemulsion synthesis commonly yields particles typically 1–50 nm in mean diameter with poor crystallinity and large size dispersions (10–35% dispersion) compared to high-temperature methods.

Hybrid nanoparticles are structures containing two or more, spatially distinct materials of varying composition. Hybrid particles thus combine the properties of these two or more functional components, and have attracted attention due to potential applications ranging from nanomedicine to catalysis. Synthesis of pure hybrid structures requires carefully tuned conditions that prevent the nucleation and growth of individual particles rather than those joined by a solid-state interface. For example, Figuerola and co-workers reported a two-step colloidal strategy to prepare bi-magnetic FePt-Fe_3O_4 heterodimers.[36] Bifunctional optical-magnetic ZnO-γ-Fe_2O_3 hybrid nanocrystals were synthesized by Yang *et al. via* layer-by-layer assembly.[37] Other bifunctional nanomaterials such as Co-CdSe[38] and FePt-CdS[39] have been reported and are predicted to be useful in medical science and biotechnology. Irudayaraj *et al.*[40] reported preparation of Fe_3O_4-Au-Fe_3O_4 "nanodumbbells" and Fe_3O_4-Au necklace-like chains to explore their functional properties and uses in magnetic resonance imaging, bioseparation, and near-IR photothermal ablation. Most recently, a general method for producing heteromultifunctional structures has been used to make *M*-Pt-Fe_3O_4 (*M* = Au, Ag, Ni, Pd) heterotrimers, M_xS-Au-Pt-Fe_3O_4 (*M* = Pb, Cu) heterotetramers, and higher-order oligomers based on a heterotrimeric Au-Pt-Fe_3O_4 building block.[41] These represent some of the most complex hybrid nanostructures reported to date. In the above examples, the complex nature of these syntheses often results in samples that contain the target hybrid structure together with individual particle impurities. In ref. 41, the yield of the target structures, based on the structures observed in electron microscopy images, varied from 90% (Pt-Fe_3O_4) to 70% (Ni-Pt-Fe_3O_4). In ref. 40 the percentage of individual iron particles is not reported but 60% of the dumbbell structures had two Fe_3O_4 domains on the Au nanoparticle, and the remaining 40% had three or more Fe_3O_4 domains. However, the majority of reports of hybrid structures do not describe the yield of hybrid particles in the overall sample.[37–39] The question of polydispersity in hybrid nanostructures is additionally complicated by the possible relative arrangements of the components in the heterostructure, uniformity in size of each component, and the presence of individual nanoparticles as impurities in the mixture.

Highly optimized syntheses of magnetic nanomaterials[42–44] have yielded samples with narrow size distributions (±10% of the mean diameter). An often-overlooked issue is the commonly observed problem of irreproducibility of these optimized synthetic conditions, which make production of similarly 'perfect' samples challenging. In addition, it is likely there are heterogeneities in composition and crystallinity within a particle sample. The roles of these types of variance within the sample on the function of a

material are unknown, although in most cases the ensemble average leads to the observed function. It is important to develop and apply methods by which particles are separated, isolated and purified so that structure-function can be elucidated. However application of analytical separations has largely been limited to micron scale particles and biological cells.[45] The remainder of this perspective describes the current methodology for nanoparticle manipulation, separation, and isolation and the abilities of these to purify nanoparticles and heterostructures.

Separation of magnetic nanoparticles by field flow fractionation

Field Flow Fractionation (FFF) methods are flow-based separation techniques to purify a range of materials including nano- and microparticles.[46] FFF uses a homogeneous external field applied orthogonal to the direction of flow to achieve efficient separation. Presently, FFF has been implemented to separate macromolecules in wide ranges of molecular weights (10^3–10^{16} Da) and particle sizes (10^{-2} to 10^2 μm), as well as organized structures such as cells and microorganisms.[47] Recent advancements in FFF have enabled improved trapping efficiency and resolution of particles with smaller sizes.[48,49] The most successful strategies for purification and separation of magnetic nanoparticles use applied magnetic fields to manipulate transport. Magnetic field FFF (MFFF) has been shown to be useful for the separation of particles by the application of an external magnetic field, which causes particle magnetization. The magnetic force thus acting on the nanoparticles is defined by:[50,51]

$$F_m = (m\cdot\nabla)B \qquad (1)$$

where m is the magnetic moment (A m^2) and ∇B is the magnetic flux gradient (T/m).

Fletcher *et al.*[52] predicted that the separation of iron oxide nanoparticles in the presence of low magnetic field gradients (<100 T/m) would be limited to particles with ~50 nm diameter or larger. These theoretical calculations predicted that the transport of particles with diameters less than 50 nm are dominated by Brownian motion and in addition, the drag force opposing particle motion cannot be overcome by the magnetic forces. However, these calculations did not reflect the single domain character of nanoparticles and ignored magnetic dipole–dipole interactions between particles. Magnetic dipole interactions could result in reversible formation of aggregates, which would have a stronger response to a magnetic field. Indeed, experimental observations of magnetic field based separations of particles with diameters smaller than 50 nm suggest that further refinement of the theory to account for interparticle coupling is necessary.

Our group demonstrated separation of different types of magnetic nanoparticles in an open tubular capillary column by use of MFFF.[53] Because the magnetic force depends on the particle magnetic moment, this technique separates magnetic nanoparticles according to size and material composition. The basic setup of the experiment is shown above in Fig. 2; samples injected into the MFFF capillary interact with the external magnetic field, which forces the particles toward higher field gradient along the accumulation wall. Material that interacts strongly with the field is therefore restricted to slower flow streams near the wall of the channel, while material that interacts weakly with the magnetic field resides toward the center of the channel. This method successfully separated a mixture of 6 nm ± 0.9 nm diameter maghemite (γ-Fe_2O_3) and 13 nm ± 1.8 nm diameter cobalt ferrite ($CoFe_2O_4$) nanoparticles into two monodisperse fractions. TEM analysis of these fractions post separation contained fractions whose particle diameters were 5.6 ± 0.9 nm and 12.5 ± 1.5 nm, respectively.

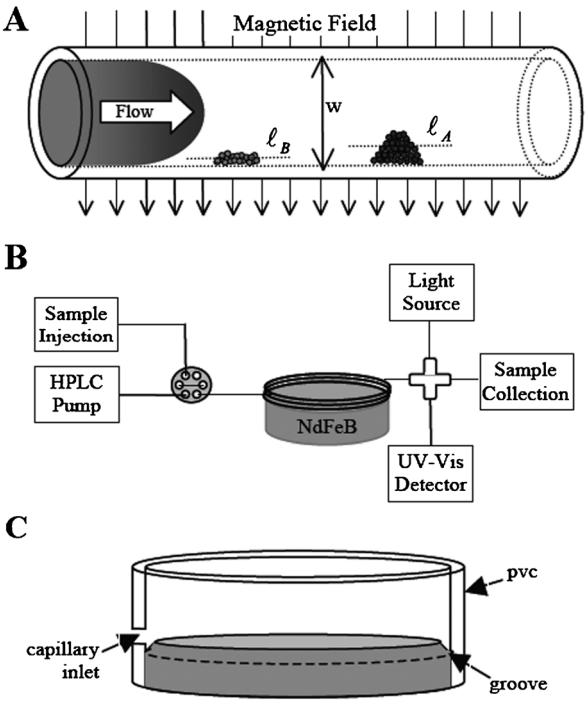

Fig. 2 (**A**) Diagram of the MFFF separation mechanism. (**B**) Schematic of the MEFF instrument. Flow is controlled by an HPLC pump and injected *via* a six-port injection valve onto a 250 μm capillary. The capillary is wound around a NdFeB magnet and elution monitored by UV-visible absorbance. (**C**) The capillary is wound around the magnet (3.81 cm in length) in the grove formed with the PVC pipe and bevelled edge of the magnet and PVC interior wall. Reprinted with permission from Williams *et al. Anal Chem.* 2005, **77**, 5055–5062. Copyright 2005 American Chemical Society.

Williams *et al.* designed a modified MFFF technique by placing the separation channel in a quadrupole magnet.[54,55] The studies investigated a commercially available sample of dextran coated magnetite with a nominal size range of 230 ± 150 nm in diameter. The quadrupole magnet apparatus revealed that 95% of the particles within the sample were 75 nm and 390 nm in diameter with a mean diameter of 178 nm. The size dispersities of these two fractions were not reported.

In an interesting study, Rheinländer *et al.* compared the efficiency of MFFF and nonmagnetic size-exclusion chromatography (SEC) to iron oxide nanoparticles.[56] Two different magnetic nanoparticles were studied: 5–6 nm diameter iron oxide nanoparticles coated with dextran and 8 nm diameter iron oxide nanoparticles with poly(ethylene glycol) modified surfaces. The samples were passed through a column packed with iron spheres (0.3 mm diameter) and the magnetic field

was altered to affect the retention of the iron oxide nanoparticles. The order of elution was found to depend on size, with the smaller iron oxides eluted first followed by the 8 nm poly(ethylene glycol) diameter nanoparticles. In contrast, SEC yielded fractions in which the average nanoparticle size *decreased* with elution time. Analysis of the fractions separated by SEC and MFFF reveals similar size distributions. However, MFFF is advantageous because it is faster and has a higher capacity.

More recently, we have developed a technique called differential magnetic catch-and-release (DMCR)[57] to separate different-sized magnetic nanoparticles. DMCR is similar to microcapillary hydrodynamic chromatography (HDC) in that it does not use a stationary phase, but like MFFF relies on an external magnetic field to effectively separate the target analyte. This method uses an electromagnet to apply a variable magnetic flux density orthogonal to the flow stream in the open tubular capillary. We demonstrated the roles of magnetic flux density and solvent flow rate on the retention of $CoFe_2O_4$ magnetic nanoparticles. Balancing the relative strength of the drag and magnetic forces enabled the separation of a polydisperse sample of 8.4 ± 1.5 nm, 12.0 ± 1.2 nm, and 17.0 ± 1.2 nm diameter $CoFe_2O_4$ nanoparticles into monodisperse fractions that are selectively released into the flow stream. For example, the original sample of 17 nm $CoFe_2O_4$ nanoparticles was loaded onto the column and a 0.5 T magnetic flux density was applied. The sample was fractionated into two peaks: the fraction not interacting with the magnetic field eluted first (12.8 ± 3.6 nm in diameter) followed by the retained fraction (16.7 ± 1.9 nm in diameter). Subsequent research investigated a series of experiments designed to further validate this approach.[58] Using mixtures of Au ($\sim$4 nm diameter) and $CoFe_2O_4$ nanoparticles (6.9 ± 1.08 nm, 10.6 ± 1.43 nm, and 16.6 ± 1.25 nm diameter, respectively) as model systems, the column loading capacity, resolution, capture yield, and effects of mobile phase viscosity on separation in DMCR were examined.

Peak resolution in DMCR is externally controlled by selectively releasing the nanoparticles at a prescribed time from the column by removing the magnet flux density. However, longer capture times increase peak resolution at the expense of the capture yield. Furthermore, the nanoparticle diameter, mobile phase velocity and viscosity, and applied magnetic field affect the nanoparticle capture yields. Using optimized parameters, a mixture of $CoFe_2O_4$ nanoparticles whose diameters were 8 and 12 nm were separated into monodisperse fractions. The elution profile for a solution of $CoFe_2O_4$ was investigated at a flow rate of 10 μL min^{-1} and magnetic field strengths of 2, 0.5, and 0.0 T. The first and second fractions to exit the capillary were 6.7 ± 1.4 nm and 8.3 ± 1.5 nm in diameter, while the final fraction to elute off the column yielded a slightly more monodisperse distribution of 11.8 nm $\pm$ 1.3 nm in diameter, respectively. When the release times were short, the relative peak areas of each separation corresponded to the relative concentrations of the particles in the original sample.

Heterostructured or hybrid nanocrystals are of increasing interest because of the enhanced chemical and physical properties when two or more inorganic materials are combined.[59] For example, core/shell nanocrystals have an inorganic material that is uniformly grown around a nanocrystal core. More elaborate approaches that have been recently reported lead to nanocrystals with finer topological control of their composition.[60–62] For example nanocrystal heterodimers contain two domains of different materials are joined together through a specific facet;[63,64] or dumbbell-shaped nanocrystals made of a semiconductor nanorod and two domains of another material (*e.g.* Au) grown on the tips of the nanorods.[65,66] To demonstrate the use of DMCR for separations of real systems, it was used to analyze and purify two different nanoparticle heterostructures Au-Fe_3O_4 and FePt-Fe_3O_4. First, DMCR facilitated the removal of individual Fe_3O_4 nanoparticle impurities from as-synthesized Au-Fe_3O_4 hybrid particles (Fig. 3), yielding a purified Au-Fe_3O_4 sample with a significantly higher magnetic moment.[67] We note that the purified heterostructures in Fig. 3d has only a small number of individual particle impurities ($\sim$3%) but still are a mixture of Au-Fe_3O_4 dimers, trimers and higher order structures. In separate experiments, analysis and purification of a FePt-Fe_3O_4 heterodimer sample identified *magnetic* polydispersity in the sample, which is defined as heterodimers with statistically identical morphology and size but different magnetic moments. After separation of these fractions, analysis revealed that the magnetic dispersity was a result of variation of Fe : Pt ratio in the FePt component of the dimers.[51]

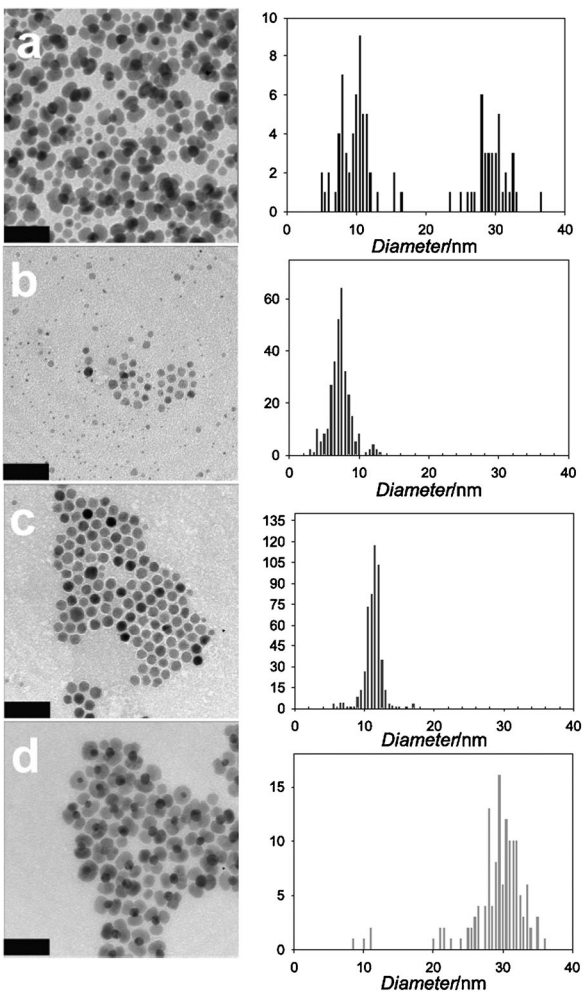

Fig. 3 TEM images and size distribution analysis of the (**A**) as-prepared Au-Fe_3O_4 and fraction (**B–D**) collected from the DMCR. Scale bars are 50 nm Reprinted with permission from Williams *et al. Angew. Chem., Int. Ed.*, 2011, **50**, 9875.

Separation and analysis of magnetic nanoparticles through porous media

Researchers have also focused on developing methods for more efficient separations of magnetic nanoparticles utilizing column flow techniques. High-gradient magnetic separation (HGMS) is an analytical technique used to isolate magnetic species from a nonmagnetic medium. HGMS most commonly uses a column packed with micron-sized magnetic wires surrounded by an electromagnet (Fig. 4).[68] When an external magnetic field is applied, the micro wires within the column magnetize, dehomogenize the field, and generate a field gradient that attracts magnetic species in solution. Magnetic species are trapped against the micro- spheres until the external field is removed or solvent forces elute them from the column. Typically, HGMS has been used to separate micron- scale or larger particles or aggregates. In some cases, magnetic nanoparticles have been used as separation agents; however, these nanoparticles have usually been present as micron-scale aggregates[69] or encapsulated in larger polymer beads.[70] The larger volume of these particles makes magnetic collection by HGMS (or other means) relatively straightforward. The application of HGMS to suspensions of individually dispersed magnetic nanoparticles (magnetic fluids) has been studied in much less depth. Hatton *et al.* studied the capture efficiency of iron oxide nanoparticles from water *via* HGMS.[52] Particle samples were either coated with a phospholipid or a polyacrylic-acid-polyethylene oxide copolymer. Although individual particles were not retained on the column, aggregates of iron oxide copolymer and phospholipids functionalized were.

Colvin *et al.*[71] illustrated separation of Fe_3O_4 nanoparticles on a column packed with steel wool and applied a tunable magnetic field ($<$ 1–2 T/m, gradients $<$100 T/m) (Fig. 5). The influence of the field on the retention time of nanoparticles with varying diameters less then 20 nm was demonstrated. Higher fields were required to retain smaller particles on the column. The dispersity of the Fe_3O_4 nanoparticles separated using this technique is approximately equivalent to the DMCR methodology for Fe_3O_4 of similar size.

Ritter's theoretical investigation[72] of a heteroflocculation model described the magnetic forces between two spherical particles: antiferromagnetic magnetite (100–500 nm radius) and adsorbate paramagnetic $Fe(OH)_2$ (20–80 nm radius). In the calculation, magnetic forces acting on the $Fe(OH)_2$ were opposed only by Brownian motion. $Fe(OH)_2$ was absorbed to

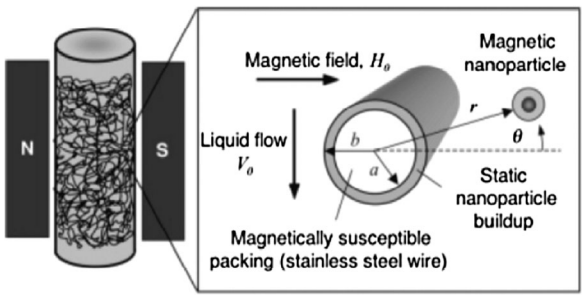

Fig. 4 Overview of the HGMS system consisting of a column packed with magnetizable wires with a radius, a, of ~50 μm. The magnetic nanoparticles build up around the wire to radius, b. Reprinted with permission from Hatton *et al. AIChe J.*, 2004, **50**, 2835.

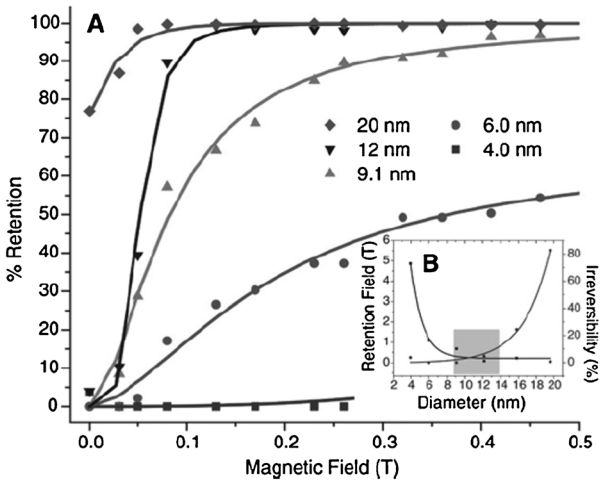

Fig. 5 (**A**) Size-dependent magnetic separation of 4.0, 6.0, 9.1, 12, and 20 nm Fe_3O_4 nanocrystals in hexane passed through a column separator packed with stainless steel wool. (**B**) The absolute field required to retain 100% of the nanocrystals loaded to the stainless steel column *vs.* the diameter of Fe_3O_4 nanocrystals. The shaded area represents the optimal size for magnetic separations. Reprinted with permission from Colvin and co-workers *Science*, 2006, **314**, 964. Copyright 2006.

the antiferromagnetic magnetite particles when the strength of the magnetic field overcame Brownian motion. This model showed that the external field strength and the size of the adsorbent and adsorbate particles are all important in HGMS. Wang and colleagues[73] experimentally studied the capture of Fe_3O_4 nanoclusters with HGMS. Longer columns, larger clusters of particles and slower velocities resulted in better capturing efficiencies. Clusters $>$50 nm diameter were efficiently captured (99.9%) at high flow rates. By increasing the column length results in increased capturing efficiency for all but the very smallest of the particles under study. Using a column of 10.5 cm in length, the eluted nanoparticles were exclusively single nanoparticles with sizes from 20 to 30 nm in diameter, even at high velocities. Nishijima and colleagues[74] captured 6 nm diameter FePt particles and 15 nm diameter Fe_3O_4 particles in a magnetic filter column. This column magnetically trapped particles by applying an external magnetic field (0.5 T or 2.0 T) to magnetize and trap the particles on a column packed with a magnetic filter made of ferromagnetic particles 0.3 mm in diameter. When the magnet field was turned off, the magnetic nanoparticles eluted from the column, and separation efficiencies of ~94% and 40% were achieved for Fe_3O_4 and FePt.

Ritter *et al.*[75] investigated the retention performance of an 80 wt% magnetite-silica composite HGMS matrix compared with traditional stainless wool with an aqueous slurry containing Fe_2O_3 nanoparticles. Overall, the magnetite-silica composite was ~30–40% less effective than stainless steel toward retaining iron oxide nanoparticles. The transport of magnetic nanoparticles in aquatic environments was studied using maghemite (γ-Fe_2O_3) and $(Fe_xNi_{1-x})_yO_z$ nanoparticles as a function of pH and particle iron content. Walker *et al.*[76] demonstrated that the transport of the nanoparticle samples was influenced by a combination of electrostatic and magnetic interactions. Nanoparticles with higher Ni content (and lower magnetic moment) were observed to

elute to a greater extent than particles with higher magnetic moment at both pH 6 and 9. The γ-Fe_2O_3 particles were most retained, which was indicative of magnetic field induced dipolar aggregation. Particle size distribution, concentration, and magnetic attraction affect transport of poly(styrene sulfonate) (PSS) Fe^0 nanoparticles in sand columns. Lowry and colleagues[77] showed at low concentrations (30 mg L^{-1}) all particles were mobile in the columns regardless of size or magnetic attractive forces. At high concentrations ($\sim$g L^{-1}), deposition of the PSS-nanoparticles ($\sim$24 nm diameter) with the lowest Fe^0 content (4 wt%) was similar to PSS-modified hematite. A polydisperse sample ($\sim$15–260 nm diameter) with an Fe^0 content between 10 to 60% was more sensitive to particle size distribution: the greater polydispersity led to higher degrees of magnetic field induced aggregation, which contributed to greater affinity on the column.

Our group[78] focused on quantifying the transport of 3, 8, and 14 nm diameter $CoFe_2O_4$ nanoparticles through alumina and polycarbonate mesoporous membranes mounted between two halves of a u-tube shaped diffusion cell. The translocation of the nanoparticles caused an increase in the absorption of the receiving solution. Using the measured extinction coefficients of the particles, the absorption values were converted to molar quantities and used to determine flux through the pores. In the absence of a magnetic field, flux decreased with increasing particle size and decreasing pore diameter. Slightly faster transport was observed in aqueous solutions than in hexane, which was unexpected because the viscosity of hexane (2.9×10^{-3} P) is smaller than the viscosity of water (8.9×10^{-3} P). However the observed differences in transport were likely due to varying degrees of wettability of the alumina *versus* polycarbonate surfaces. The impact a magnetic flux gradient on permeation was also explored. For larger membrane pore diameters, applied magnetic fluxes increased the rate of transport of 14 nm diameter $CoFe_2O_4$ particles more than that of 3 or 8 nm diameter particles, reflecting their differences in magnetic susceptibility. As the pore diameter decreased, larger particles were excluded from the membrane. The magnetic field apparently induced dipole–dipole interactions that led to formation of aggregates with sizes equal or larger than the pore diameter. The results further pointed to magnetic-induced aggregation of larger $CoFe_2O_4$ particles while in the magnetic field which impede transport through porous membranes, but suggested opportunities for using this to obtain size-selective separations.

Subsequent research[79] investigated intermolecular interactions of $CoFe_2O_4$ nanoparticles with alumina membranes functionalized with trimethoxysilanes. Increased fluxes, compared to untreated membranes, were observed when the membranes were modified with the siloxanes. However the flux decreased in both hexane and aqueous solutions when the length of the hydrocarbon chains lining the interior walls of the membrane increased. The rate and selectivity of transport of the permeating nanoparticles were also affected by the terminal head groups (*e.g.* –Br, $-NH_2$, –COOH) on the hydrocarbon chains. This report demonstrated that both the pore and particle surface chemistries play important roles in flux and permeability, provide the initial framework to study transport in increasingly complex environments, and suggested modifications that further enable nanoparticle separation and analysis.

Magnetic nanoparticle separation in micro-channels

Microfluidic, or "lab on a chip", devices are an enormous research area because of their promise for the rapid analysis of exceedingly small quantities of reagents with high resolution in systems that should prove to be both low in cost and portable.[80] The unifying goal of micro total analysis systems (μTAS) is to develop the ability to perform complex combinations of analytical and chemical functions, including separation and detection of samples, on a single disposable chip. The majority of research utilizing magnetic fields and micro channels has focused on separating and detecting biomolecules and cells in a ferrofluid. Although less intensely studied in μTAS applications, nanoparticle-based technologies have the potential to play a significant role. In particular, the superparamagnetic behavior of nanoscale particles at room temperature makes them outstanding candidates for incorporation in μTAS devices.

Numerical simulations serve as an investigative tool to probe the design parameters in microfluidic systems that include flow velocity, channel dimensions, geometries and nanoparticle properties which all influence the development of microdevices. Zhou *et al.*[81] developed a mathematical model for predicting the transport and capture of multiple magnetic nanoparticles in a microfluidic system consisting of a microchannel enclosed by a permanent magnet. It was demonstrated that both size and point of release within the microchannel of 50 nm diameter magnetic nanoparticles affects capture. It was further shown that the angular position of the magnet around the microchannel is critical for optimal trapping efficiency.

Sonkusale *et al.* utilized a low power AC susceptometer to simultaneously detect multiple magnetic nanoparticles in solution.[82] AC magnetic susceptometry is a precise detection technique that capitalizes on the diffusive properties of magnetic nanoparticles in solution[83,84] and may be appropriate for point-of-care diagnostics with potential for chip implementation.[85] The measurement of AC susceptibility for individual iron oxide nanoparticles (size range 15–50 nm diameter) under an external magnetic field (0.5 mT) showed the complex magnetic susceptibility to be inversely proportional to the effective hydrodynamic size of the iron oxide nanoparticles. Sonkusale further demonstrated that multiplex detection for mixtures of differently sized magnetic nanoparticles by measuring the change in Brownian relaxation. Iron oxide nanoparticles with diameters of 25 and 50 nm diameter were successfully separated as indicated by their measured frequencies. Although this technique is efficient at separating magnetic nanoparticles, higher AC susceptometer sensitivity is needed to differentiate between nanoparticles that statistically overlap in size by adjacent frequency peaks.

Our group[86] studied the ability to move, manipulate, and inject magnetic nanoparticles between a cross-channel microfluidic device. Two orthogonal channels were prepared using PDMS and pressure-driven flow delivered the mobile phase (Fig. 6). The ability to magnetically manipulate Fe_2O_3, and $CoFe_2O_4$ nanoparticles within micrometre-sized channels was investigated. Nanoparticles translocating through and between flow streams was monitored using an absorption detector. Placement of an external magnet beneath the cross-channels increased the transfer of magnetic particles between flow streams

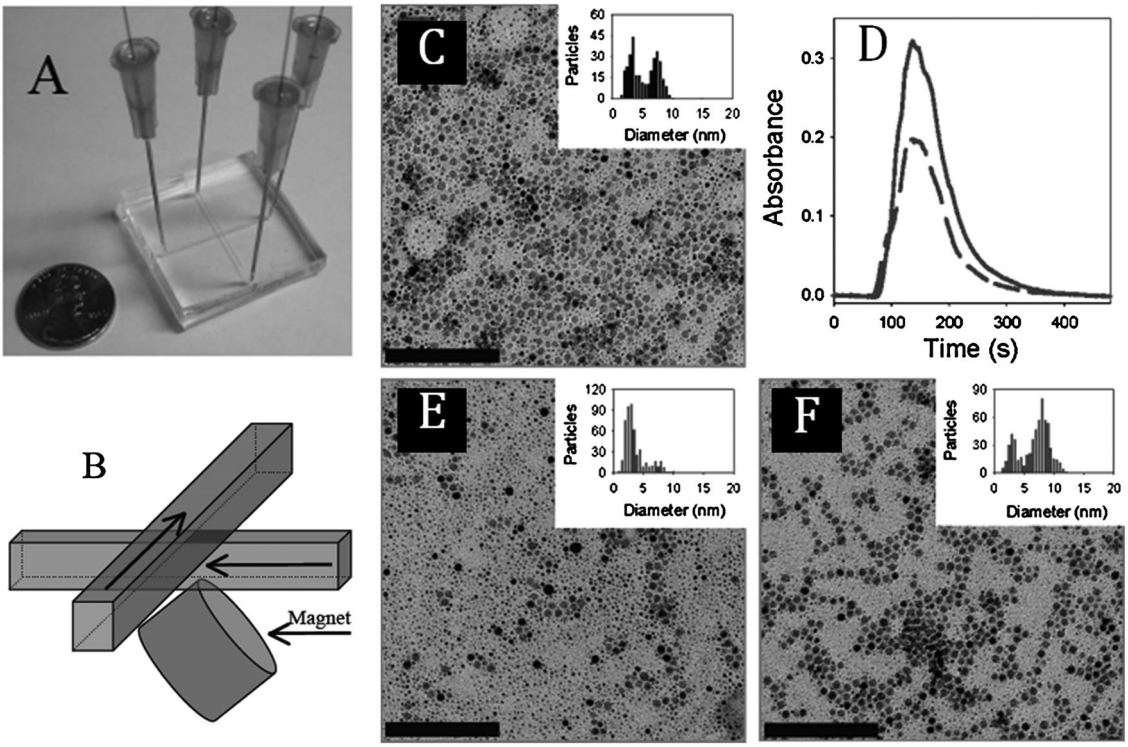

Fig. 6 (**A**) PDMS crossed-microchannel. (**B**) Diagram of the crossed channels with arrows indicating direction of fluid flow with a NdFeB permanent magnet placed at the channel intersection. (**C**) TEM image of the Au and Fe_2O_3 nanoparticle mixture. (**D**) Absorbance v. time of the upper channel with (---) and without (-) a magnetic field and a flow rate of 15 μL min^{-1}. (**E**) and (**F**) Representative TEM images of the separated nanoparticle fractions in the presence of a magnet. Scale bars are 100 nm. Reprinted with permission from Williams *et al. Anal. Chem.*, 2007, **79**, 5746–5753. Copyright 2007 American Chemical Society.

but nonmagnetic Au nanoparticles were not affected by the magnetic field. Varying the magnet position periodically pulled the magnetic nanoparticles into the lower flow stream. The magnetic transfer of the nanoparticles was also related to the solvent flow rate; as the velocity decreased, the amount of particles that exited in the lower channel increased. Thus, transfer efficiency depended on the relative velocity in the laminar upper stream *versus* downward velocity of motion due to magnetic attraction. Luo *et al.*[87] similarly manipulated co-precipitated Fe_3O_4 nanoparticles dispersed in water that was sheared into picolitre-volume droplets by the oil-phase in a T-junction PDMS microchannel. In the absence of a magnetic field the nanoparticles exited the upper-most outlet due to laminar flow, however they are deflected using a perpendicular magnetic field. The results showed that the deflection to selective outlet channels was proportional to the magnetic field gradient and magnetic nanoparticle concentration, as well as magnetic position.

Descroix and co-workers[88] developed a microchip for the efficient trapping and release of 30 nm diameter maghemite nanoparticles. The microdevice was comprised of micron sized iron beads (6–8 μm diameter) packed in a channel that were used to focus magnetic field lines from an external magnet and generate local high magnetic gradients. Due to the small size of the nanoparticles, a high magnetic flux gradient was required for magnetic trapping. Numerical simulations and experimental results showed preferentially trapped maghemite at the iron bead magnetic poles, where the magnetic force is increased by 3 orders of magnitude. The capture capacity, which is defined as the maximal amount of magnetic nanoparticles using such a magnetic chamber, was determined to be 1.1×10^4 μm^{-3} at flow rates of 10, 50, and 100 μL h^{-1}. The capacity of capture is not affected by the flow rate illustrating that the magnetic force generated is still higher than the drag force.

Magnetic nanoparticle separation in electric fields

Capillary electromigration methods are of increasing use for analytical separations and characterization of nanoparticles. These methods fractionate dispersions according to differences in the particle size or measure the electrophoretic mobilities. Electromigration can provide information to characterize surface charge density and size while also offering further detail of their chemical composition. For example, electrophoretic mobilities are converted to zeta potentials (ζ) and retardation coefficient (κR, where R is the particle radius and κ the reciprocal Debye length) values.[89]

Capillary electrophoresis (CE) has been used for the separation of inorganic colloidal nanoparticles including silica,[90] gold,[91] silver,[92] and gold/silver core/shell[93] nanoparticles. Interest has now shifted to metal oxide mixtures including iron oxide. Morneau *et al.*[94] used CE to characterize ferrofluids (magnetic iron oxide particles ranging from 30–200 nm diameter) that differed in stabilizing surface groups but were mainly anionic. More recently, d'Orlye *et al.*[95] characterized populations of maghemite particles (6–10 nm diameter) suspended in acidic,

citrate, or basic aqueous media. The capillary walls were coated to prevent adsorption of the cationic nanoparticles to the surface, and the migration times and peak shapes were shown to depend on the capillary surface chemistry. The optimal coating was determined to be didodecyldimethyl-ammonium bromide, which yielded a decrease in particle electrophoretic mobility and gave Gaussian-shaped peaks. However CE can be experimentally challenging and requires specialized equipment because of the high electric fields that are required, and the need to optimize both the mobile phase (*e.g.* pH, ionic strength, *etc.*) and capillary surface chemistry. These can be particularly problematic for nanoparticle separations since changes in solvent and surface chemistry can lead to aggregation, shear degradation, or capillary adsorption. In addition, the pH of a chosen buffer in CE can modify particle charge and dispersibility.[34]

Electrical Field-Flow Fractionation (ElFFF) separates analytes based on their electrophoretic mobility and size but without the drawbacks of CE.[34,96–98] The smaller electrical field (0 to 2 V) and range of channel dimensions (several μm) in ElFFF significantly reduce the risk of particle damage.[99] Moreover, the mobile phase is generally water, eliminating some of the complications of using buffers with nanoparticles.[100] The simplicity of design and ease of use makes ElFFF a promising technique for separation of nanoscale particles. Cyclical FFF is reported to separate particles based on their migration rates, which depend on transport coefficients.[101] In cyclical FFF the direction of the electric field is alternated according to a periodic or cyclic pattern during the course of separation. Recently, a cyclical electrical FFF (CyElFFF) has been developed.[102,103] The reported explanation for CyElFFF was that the alternating current short circuits the large capacitance associated with the parallel plate channel electrodes as the frequency increases. In addition, the high voltages (> 1.7 V) induce water electrolysis and bubble formation, which is problematic bubble formation in ElFFF. However the higher frequencies of CyElFFF generate fewer or bubbles, enabling separations with higher applied voltages.

Lespes and colleagues[82] investigated different operating parameters in CyElFFF to evaluate their effect on the retention mechanisms and fractionation power for Fe_3O_4 nanoparticles in a wide range of size (*i.e.* 20–400 nm diameter) and electrophoretic mobility. The highest separation efficiency was investigated as a function of voltage, frequency, flow rate, and stop flow influence. Dragiciu *et al.*[104] controlled the fluid flow of aqueous solutions with different nanoparticles such as Fe_3O_4, Au, Fe_3O_4-Ag and Fe_3O_4-Au by an array of Cr/Au electrodes. The crystals of magnetite nanoparticles used in this experiment were 10 nm in diameter. The electrodes were used to apply a voltage (1.5 to 5 V) across the solution. The particles migration started at 2.5 V and Fe_3O_4-Au responded most strongly with the applied voltage. Future work separating nanomaterials by way of electric fields shows great promise. Although current research has proven to be efficient for isolating nanoparticle samples, further development needs to focus nanoparticles smaller than 20 nm, since this size regime is particularly important for biomedical applications.

Conclusions

The role of size and shape uniformity of nanoparticle systems in the overall function of a nanomaterial is largely unknown because despite advances in synthesis, there remain few analytical methods for producing pure, monodisperse nanoparticle samples. In some applications, polydispersity—of size, shape, crystallinity, or composition—may not be a hindrance. However for some emerging applications, particularly in biomedical areas, obtaining and confirming the purity of the nanoparticle or particle heterostructure is centrally important.

The majority of wet synthetic methods yield size polydisperse samples, and even in the best and most highly optimized approaches, there may be polydispersity of composition and crystallinity within a particle sample that has monodisperse shape and size. In comparison with the body of literature reporting synthesis of nanoparticulate materials, there is comparatively little reported for analytical tools to separate, isolate, purify and analyze magnetic particles. This article catalogues a set of separation techniques that are the initial steps toward purification and analysis of magnetic nanomaterials. However, clearly more and better methodologies are needed to push the limits of the ability to make truly size and function monodisperse samples. High-throughput methods that would be useful for purification and analysis of magnetic nanoparticle based chemotherapeutics and diagnostic imaging are essential. We view this as a challenge to physical chemists and separation scientists to address this critical need that ultimately would be enabling for the real use and application of magnetic nanoparticles.

Notes and references

1 G. Schmid, *Nanoparticles: From Theory to Application*, Wiley-VCH, Weinheim, 2004.
2 K. J. Klabunde, *Nanoscale Materials in Chemistry*, Wiley-Interscience, New York, 2001.
3 J. Park, K. An, Y. Hwang, J. G. Park, H. J. Noh, J. Y. Kim, J. H. Park, N. M. Hwang and T. Hyeon, *Nature Mater.*, 2004, **3**, 891.
4 T. Hyeon, S. S. Lee, J. Park, Y. Chung and H. B. Na, *J. Am. Chem. Soc.*, 2001, **123**, 12798.
5 S. J. Park, S. Kim, S. Lee, Z. G. Khim, K. Char and T. Hyeon, *J. Am. Chem. Soc.*, 2000, **112**, 8581.
6 C. B. Murray, C. R. Kagan and M. G. Bawendi, *Annu. Rev. Mater. Sci.*, 2000, **30**, 545.
7 A. L. Rogach, D. V. Talapin, E. V. Shevchenko, A. Kornowski and M. Haase, *Adv. Funct. Mater.*, 2002, **12**, 653.
8 L. M. Demers, S. J. Park, T. A. Taton, Z. Li and C. A. Mirkin, *Angew. Chem. Int. Ed.*, 2001, **40**, 3071.
9 R. J. Macfarlane, B. Lee, M. R. Jones, N. Harris, G. C. Schatz and C. A. Mirkin, *Science*, 2011, **334**, 205.
10 T. Teranshi and M. Miyake, *Chem. Mater.*, 1998, **10**, 594.
11 M. P. Pileni, *Nat. Mater.*, 2003, **2**, 145.
12 S. H. Sun and H. Zeng, *J. Am. Chem. Soc.*, 2002, **124**, 8204.
13 Y. G. Sun and Y. N. Xia, *Science*, 2002, **298**, 2176.
14 L. Manna, E. C. Scher and A. P. Alvisatos, *J. Am. Chem. Soc.*, 2000, **122**, 12700.
15 D. A. Walker, K. P. Browne, B. Kowalcyck and B. A. Grzybowski, *Angew. Chem. Int. Ed.*, 2007, **46**, 8363.
16 R. Klajin, A. O. Pinchuk, G. C. Schatz and B. A. Grzybowski, *Angew Chem. Int. Ed.*, 2010, **49**, 6760.
17 F. Tao, M. E. Grass and Y. W. Zhang, *J. Am. Chem. Soc.*, 2010, **132**, 8697.
18 J. M. Yan, X. B. Zhang and T. J. Akita, *J. Am. Chem. Soc.*, 2010, **132**, 5326.
19 V. Mazumder, M. F. Chi, K. L. More and S. H. Sun, *J. Am. Chem. Soc.*, 2010, **132**, 7848.
20 Y. J. Kang and C. B. Murray, *J. Am. Chem. Soc.*, 2010, **132**, 7568.
21 M. P. Mallin and C. J. Murphy, *Nano. Lett.*, 2002, **2**, 1235.
22 E. Ruckenstein and Z. F. Li, *Adv. Colloid Interface*, 2005, **24**, 4529.

23 R. Klajin, J. F. Stoddart and B. A. Grzbowski, *Chem. Soc. Rev.*, 2010, **39**, 2203.
24 W. Maneeprakon, W. A. Malik and P. O'Brien, *J. Am. Chem. Soc.*, 2010, **132**, 1780.
25 Y. H. Wei, K. J. M. Bishop and J. Kim, *Angew. Chem. Int. Ed.*, 2009, **48**, 9477.
26 H. Wang, D. W. Brandl, P. Nordlander and N. J. Halas, *Acc. Chem. Res.*, 2007, **40**, 53.
27 A. Taleb, C. Petit and M. P. Pileni, *Chem. Mater.*, 1997, **9**, 950.
28 C. B. Murray, D. J. Norris and M. G. Bawendi, *J. Am. Chem. Soc.*, 1993, **115**, 8706.
29 V. K. Lamer and R. H. Dinegar, *J. Am. Chem. Soc.*, 1950, **72**, 4847.
30 S. Sun, H. Zeng, D. B. Robinson, S. Raox and P. M. Rice, *J. Am. Chem. Soc.*, 2004, **126**, 279.
31 T. Hyeon, S. S. Lee, J. Parl, Y. Chung and H. B. Na, *J. Am. Chem. Soc.*, 2001, **123**, 12798.
32 M. Chem, J. P. Liu and S. Sun, *J. Am. Chem. Soc.*, 2004, **126**, 8394.
33 S. Laurent, D. Forge, M. Port, A. Roch, C. Robic, L. Vander Elst and R. N. Muller, *Chem. Rev.*, 2008, **108**, 2064.
34 K. Wikander, C. Petit, K. Holmberg and M. P. Pileni, *Langmuir*, 2006, **22**, 4863.
35 D. Polli, I. Lisiecki, H. Portales, G. Cerullo and M. P. Pileni, *ACS Nano*, 2011, **5**, 5785.
36 A. Figuerola, A. Fiore, R. D. Corato, A. Falqui and C. Gianninni, *J. Am. Chem. Soc.*, 2008, **130**, 1477.
37 P. Wu, N. Du, H. Zhang, L. Jin and D. Yang, *Mater. Chem. Phys.*, 2010, **124**, 908.
38 H. Kim, M. Acherman, L. P. Balet, A. Hollingsworth and V. I. Klimov, *J. Am. Chem. Soc.*, 2005, **127**, 544.
39 S. L. He, H. W. Zhang, S. Delikani, Y. L. Qin, M. T. Swihart and H. Zeng, *J. Phys. Chem. C*, 2009, **113**, 87.
40 J. Irudayaraj and C. Wang, *Small*, 2010, **6**, 283.
41 M. R. Buck, J. F. Bondi and R. E. Schaak, *Nature Chem.*, 2012, **4**, 37.
42 D. Ho, X. L. Sun and S. H. Sun, *Acc. Chem. Res.*, 2011, **44**, 875.
43 C. Yang, J. Wu and Y. Hou, *Chem. Commun.*, 2011, **47**, 5130.
44 T. D. Schladt, K. Schneider, H. Schild and W. Tremel, *Dalton Trans.*, 2011, **40**, 6315.
45 (*a*) N. Pekas, M. Granger, M. Tondra, A. Popple and M. D. Porter, *J. Magn. Magn. Mater.*, 2005, **293**, 584; (*b*) M. Zborowski, C. B. Fuh, R. Green, L. Sun and J. J. Chalmers, *Anal. Chem.*, 1995, **67**, 3702; (*c*) S. Ostergard, G. Blakenstein, H. Dirac and O. Lesitiko, *J. Magn. Magn. Mater.*, 1999, **194**, 156.
46 M. E. Schimpf, K. Caldwell and J. C. Giddings, *Field Flow Fractionation Handbook*, Wiley-IEEE, 2000.
47 O. N. Katasonova and P. S. Fedotov, *J. Anal. Chem.*, 2009, **64**, 212.
48 I. Roemer, T. A. White, M. Baalousha, K. Chipman, M. R. Viant and J. R. Lead, *J. Chromatogr., A*, 2011, **1218**, 4226.
49 A. R. Poda, A. J. Bednar, A. J. Kennedy, A. Harmon, M. Hull, D. M. Mitrano, J. F. Ranville and J. Steevens, *J. Chromatogr., A*, 2011, **1218**, 4219.
50 M. Zborowski, L. Sun, L. R. Moore, P. S. Williams and J. L. Chalmers, *J. Magn. Magn. Mater.*, 1999, **194**, 224.
51 M. A. M. Gijs, *Microfluid. Nanofluid.*, 2004, **1**, 22–40.
52 D. Fletcher, *IEEE Trans. Magn.*, 1991, **27**, 3655.
53 A. H. Latham, R. S. Frieta, P. Schiffer and M. E. Williams, *Anal. Chem.*, 2005, **77**, 5055.
54 F. Carpino, M. Zboroski and P. S. Williams, *J. Magn. Magn. Mater.*, 2007, **311**, 383.
55 F. Carpino, M. Zborozski, L. R. Moore, J. J. Chalmers and P. S. Williams, *J. Magn. Magn. Mater.*, 2005, **293**, 546.
56 T. Rheinländer, R. Kotitz, W. Weitschies and W. Semmler, *Colloid Polym. Sci.*, 2000, **278**, 259.
57 J. S. Beveridge, J. R. Stephens, A. H. Latham and M. E. Williams, *Anal. Chem.*, 2009, **81**, 9618.
58 J. S. Beveridge, J. R. Stephens and M. E. Williams, *Analyst*, 2011, **136**, 2564.
59 P. D. Cozzoli, T. Pellegrino and L. Manna, *Chem. Soc. Rev.*, 2006, **35**, 1195.
60 B. O. Dabbousi, J. RodriquezViejo, F. V. Miulec, J. R. Heine, H. Mattoussi, R. Ober, K. F. Jensen and M. G. Bawendi, *J. Phys. Chem. B*, 1997, **101**, 9463.
61 X. G. Peng, M. C. Schlamp, A. V. Kadavanich and A. P. Alivisatos, *J. Am. Chem. Soc.*, 1997, **119**, 7019.
62 Y. W. Cao and U. Banin, *J. Am. Chem. Soc.*, 2000, **122**, 9692.
63 H. W. Gu, R. K. Zheng, X. X. Zhang and B. Xu, *J. Am. Chem. Soc.*, 2004, **126**, 5664.
64 H. W. Gu, Z. M. Yang, J. H. Gao, C. K. Chang and B. Xu, *J. Am. Chem. Soc.*, 2005, **127**, 34.
65 T. Mokari, C. G. Sztrum, A. Salant, E. Rabani and U. Banin, *Nat. Mater.*, 2005, **4**, 855.
66 T. Mokari, E. Rothenberg, I. Popov, R. Costi and U. Banin, *Science*, 2004, **304**, 1787.
67 J. S. Beveridge, M. R. Buck, J. F. Bondi, R. Misra, P. Schiffer, R. E. Schaak and M. E. Williams, *Angew. Chem., Int. Ed.*, 2011, **50**, 9875.
68 G. D. Moeser, K. A. Roach, W. H. Green, P. E. Laibanis and T. A. Hatton, *AIChE J.*, 2004, **50**, 2835.
69 J. J. Hubbuch and O. R. T. Thomas, *Biotechnol. Bioeng.*, 2002, **79**, 301.
70 D. Leun and A. K. Sengupta, *Environ. Sci. Technol.*, 2000, **34**, 3276.
71 C. T. Yavuz, J. T. Mayo, W. W. Yu, A. Prakash, J. C. Falkner, S. Yean, L. Cong, H. J. Shipley, A. Kan, M. Tomson, D. Natelson and V. L. Colvin, *Science*, 2006, **314**, 964.
72 A. D. Ebner, H. J. Ploehn and J. A. Ritter, *Sep. Purif. Technol.*, 1997, **11**, 199.
73 A. Ditsch, S. Lindenmann, P. E. Laibinis, T. A. Hatton and D. I. C. Wang, *Ind. Eng. Chem. Res.*, 2005, **44**, 6424.
74 R. Nako, Y. Matuo, F. Mishima, T. Taguchi and S. J. Nishijima, *J. Phys.: Conf. Ser.*, 2009, **156**, 012032.
75 A. D. Ebner and J. A. Ritter, *Sep. Purif. Technol.*, 2004, **39**, 2863.
76 Y. Hong, R. J. Honda, N. V. Myung and S. L. Walker, *Environ. Sci. Technol.*, 2009, **43**, 8834.
77 T. Phenrat, H. H. Kim, F. Fagrlund, T. Illangasekare, R. D. Tilton and G. V. Lowry, *Environ. Sci. Technol.*, 2009, **43**, 5079.
78 J. R. Stephens, J. S. Beveridge, A. H. Latham and M. E. Williams, *Anal. Chem.*, 2010, **82**, 3155.
79 J. R. Stephens, J. S. Beveridge and M. E. Williams, *Analyst*, 2011, **136**, 3797.
80 (*a*) P. A. Auroux, D. Iossifidis, D. R. Reyes and A. Manz, *Anal. Chem.*, 2002, **74**, 2637; (*b*) T. Vilkner, D. Janasek and A. Manz, *Anal. Chem.*, 2004, **76**, 3373.
81 A. Munir, J. Wang and H. S. Zhou, *IET Nanobiotechnol.*, 2009, **3**, 55.
82 K. Park, T. Harrah, E. B. Goldberg, R. P. Guertin and S. Sonkusale, *Nanotechnology*, 2011, **22**, 085501.
83 S. H. Chung, A. Hoffmann, S. D. Bader, C. Liu, B. Kay, L. Makowski and L. Chen, *Appl. Phys. Lett.*, 2004, **85**, 2971.
84 S. H. Chung, A. Hoffmann, K. Guslienko, S. D. Bader, C. Liu, B. Kay, L. Makowski and L. Chen, *J. Appl. Phys.*, 2005, **97**, 10R101.
85 J. J. Makiranta, J. O. Lekkala, *IEEE. EMBC*: *27th Int. Ann. Conf.*, 1256.
86 A. H. Latham, A. N. Tarpara and M. E. Williams, *Anal. Chem.*, 2007, **79**, 5746.
87 K. Zhang, Q. Liang, S. Ma, X. Mu, P. Hu, Y. Wang and G. Luo, *Lab Chip*, 2009, **9**, 2992.
88 B. Teste, F. Malloggi, A.-L. Gassner, T. Georgelin, J.-M. Siague, A. Varenne, H. Girault and S. Descroix, *Lab Chip*, 2011, **11**, 833.
89 R. J. Hunter, *Foundation of Colloid Science*, 2nd edn, Oxford University Press, New York, 2001.
90 R. M. Mcormick, *J. Liq. Chromatogr.*, 1991, **14**, 939.
91 F. K. Liu, Y. Y. Lin and C. H. Wu, *Anal. Chim. Acta*, 2005, **528**, 249.
92 F. K. Liu, F. H. Ko, P. W. Huang, C. H. Wu and T. C. Chu, *J. Chromatogr., A*, 2005, **1062**, 139.
93 F. K. Liu, M. H. Tsai, Y. C. Hsu and T. C. Chu, *J. Chromatogr., A*, 2006, **1133**, 340.
94 A. Morneau, V. Pillai, S. Nigam and F. M. Winnik, *Colloids Surf., A*, 1999, **154**, 295.
95 F. d'Oryle, A. Varenne and P. Gareil, *Electrophoresis*, 2008, **29**, 3768.
96 N. Tri, K. Caldwell and R. Beckett, *Anal. Chem.*, 2000, **72**, 1823.
97 T. Edwards, K. B. Gale and A. Bruno Frazier, *Biomed. Microdevices*, 2001, **3**, 211.
98 M.-H. Chang, D. Dosev and I. M. Kennedy, *Sens. Actuators, B*, 2007, **124**, 172.
99 M. Song, H. Sun, M. Charmachi, P. Wang, Z. Zhang and M. Faghri, *Microsyst. Technol.*, 2010, **16**, 947.
100 J. Gigault, B. K. Gale, I. Le Hecho and G. Lespes, *Anal. Chem.*, 2011, **83**, 6565.
101 J. C. Giddings, *Anal. Chem.*, 1986, **58**, 2052.
102 B. K. Gale and M. Srinvas, *Electrophoresis*, 2005, **26**, 1623.
103 A. Kantak, S. Merugu and K. B. Gale, *Electrophoresis*, 2006, **27**, 2833.
104 L. Dragiciu, M. Carp, L. Eftime, I. Stanciu and R. Müller, *Mater. Sci. Eng., B*, 2010, **169**, 186.